Article:
Bateman, M.D., Thomas, D.S.G. and Singhvi, A.K. (2003) Extending the aridity record of the Southwest Kalahari: current problems and future perspectives. Quaternary International, 111 (1). pp. 37-49. ISSN: 1040-6182

https://doi.org/10.1016/S1040-6182(03)00013-2

Bateman *et al.* (2003) as published in Quaternary International 111 (2003) 37–49

Extending the aridity record of the Southwest Kalahari: current problems and future perspectives.

Mark D. Bateman [1*], David S.G. Thomas [1] and Ashok K. Singhvi [2]

[1] Sheffield Centre for International Drylands Research, Department of Geography, University of Sheffield, Winter St., Sheffield S10 2TN, United Kingdom.
[2] Earth Science Division, Physical Research Laboratory, Ahmedabad 380 009, India.

** Corresponding Author, e-mail: m.d.bateman@sheffield.ac.uk, Tel: +44 114 222 7929, Fax: +44 279 7912*

Abstract

An extensive luminescence based chronological framework has allowed the reconstruction of expansions and contractions of the Kalahari Desert over the last 50 ka (Thomas and Shaw, 2003). However, this chronology is largely based on near surface pits and sediment exposures. These are the points on the landscape most prone to re-activation and resetting of the luminescence dating 'clock'. This is proving to be a limiting feature for extending palaeoenvironmental reconstructions further back in time. One way to obviate this is to sample desert marginal areas that only become active during significant arid phases. An alternative is to find and sample deep stratigraphic exposures. The Mamatwan manganese mine at Hotazel in the SW Kalahari meet both these criteria. Luminescence dating of this site shows the upper sedimentary unit to span at least the last 60 ka with tentative age estimates from underlying cemented aeolian units dating back to the last interglacial and beyond. Results from Mamatwan are comparable to new and previously published data from linear dunes in the SW Kalahari but extend back much further. Analysis of the entire dataset of luminescence ages for the SW Kalahari brings out important inferences that suggests that different aeolian forms, 1) have been active over different time scales in the past, 2) have different sensitivities to environmental changes and 3) have different time scales over which they record and preserve the palaeoenvironmental record. This implies that future OSL work and palaeoenvironmental reconstructions must consider both site location and its relationship to desert margins and sediment depositional styles, so that the resolution and duration of the aridity record can be optimally understood.

1. Introduction

The Mega Kalahari of southern Africa covers an area of approximately 2.5 million km^2 (Cooke, 1958; Thomas and Shaw, 1991). Spatially the Mega Kalahari extends from the Northern Cape Province of South Africa to the Congo in the north and from Namibia in the west to Zimbabwe in the east. The geomorphic processes operative within the Mega Kalahari have varied in response to climate changes through time (e.g. Thomas and Shaw 2003) and holds the potential to provide a long and detailed record of southern hemisphere Quaternary changes. From a Quaternary palaeoenvironmental perspective its significance accrues from its geological origins and its location at the juxtaposition of central southern African climatic systems. At present, relatively limited palaeoenvironmental data is available, principally due to the paucity of organic material that can be radiocarbon dated.

The Kalahari is principally formed in the structurally downwarped basin of interior southern Africa which has acted as a sedimentary sump since the Tertiary period. In places, these sediments, collectively known as the Kalahari Group, have significant thicknesses. In Etosha Basin, Northern Namibia, more than 450 m of sediments exist (Haddon, 1999). The Kalahari Group is dominated by sands principally of aeolian derivation. However the evolving endoreic drainage, of which the Okvango is the last major vestige, coupled with its generally flat surface at 900-1200m a.s.l. has allowed the redistribution, primarily by fluvial and lacustrine processes, of material eroded from the basin rim. Geomorphically the landscape of the northern and southwestern Kalahari is dominated by linear dunes, which in the case of the latter indicate a net sediment transfer from NW to SE (Fig. 1).

The Kalahari region currently experiences a marked southwest-northeast rainfall gradient and only the southwest Kalahari can be classified as true

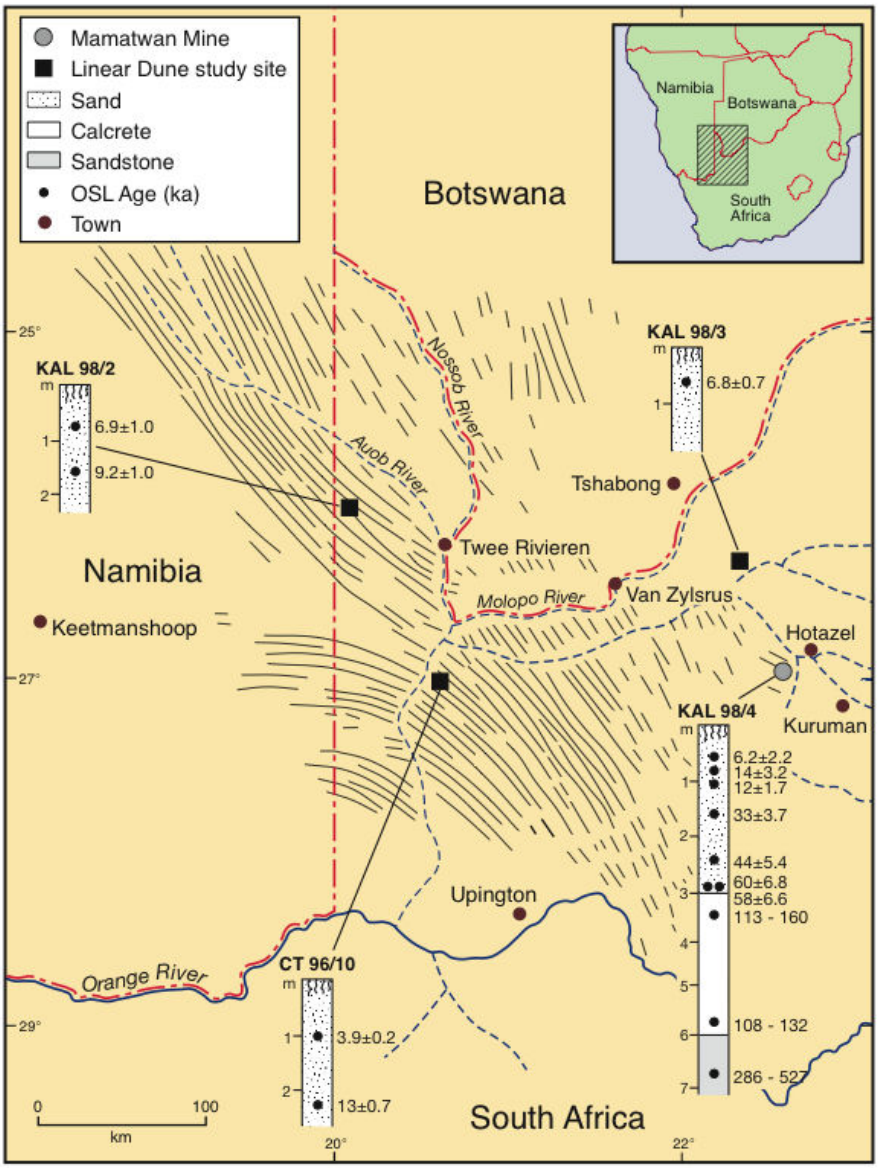

Figure 1. Map showing the linear dunes of the SW Kalahari, the study sites and OSL age estimates from this study.

desert (mean annual rainfall around 100 mm and inter-annual variability up to 55%). The rainfall gradient and variability reflect the sensitivity of the climate to the subtle changes in position of the South African anticyclone (part of the subtropical high pressure belt) and the Inter Tropical Convergence Zone (ITCZ). Such variability also reflects changes in the ability to draw moisture behind the ITCZ from the Indian Ocean in the summer and the abundance, strength, and position of winter low pressure cells from the southern Atlantic, which contribute periodic rainfall to this predominantly summer rainfall area. The influence of the ITCZ position and Indian Ocean monsoon penetration mean that the eastern extremes of the Mega Kalahari are its wettest areas, with Victoria Falls, Zimbabwe having a mean annual rainfall value of 750 mm. Rainfall variability and anomalies at decadal and multi-decadal scales (Tyson, 1986) have been linked to cyclical events including El Nino, and possibly relate to Africa-wide events that display hemispheric synchronicity (Nicholson, 2000). On millennial timescales, orbital forcing (solar isolation receipt) is now regarded as a critical driver of ITCZ-related monsoon changes and rainfall changes in the southern African summer rainfall zone (Stokes et al., 1997a; Partridge et al., 1997; Marret et al., 2001).

2. Environmental and climate change in the southern African interior

2.1 Introduction

In the Kalahari, as with other regions, a critical issue is the careful selection, evaluation and dating of suitable proxies for identifying significant precipitation changes at the millennial scale. Without this, palaeodata lacks integrity for use in climate modelling (Kohfield and Harrison, 2000). Lacustrine and pollen records have yielded valuable data from north and east Africa (e.g. Peyron et al., 2000), but these are largely absent in the southern interior of the continent. Long records, although limited both in terms of number and spatial coverage, do exist. These include the tufa-based record from the Gaap Escarpment, spanning approximately the last 250 ka (Butzer et al., 1978) and Pretoria Salt Pan (Partridge et al., 1997) spanning back to 220 ka. Data from the latter has proved instrumental in current debates of the role of orbital insolation forcing in both subtropical North and South African climate. However, this site relies on an orbitally tuned radiocarbon chronology for the first 43 ka BP and a basal fission-track date of 220 $\pm$ 52 ka and has no age control in between these points.

Aeolian deposits dominate the Kalahari and, since the 1990s, the application of luminescence dating techniques have helped palaeoenvironmental reconstruction(e.g. Stokes et al*.,* 1997a; Thomas et al*.,* 2000; Eitel and Blumel, 1998). Lancaster's (1981) original three-fold model of regional Late Quaternary linear dune building in the Kalahari has now been tested and amended accordingly. Based on approximately 50 luminescence ages, Stokes et al. (1997a; 1997b) and Thomas et al. (1997) provided a first order event chronology, and suggested episodic aeolian activity during *c.* 115-95, 46-41, 26-20 and 16-9 ka. Subsequently, an extensive and spatially diverse dating programme has been carried out (e.g. Lawson, 1998; O'Connor and Thomas, 1999; Thomas and Shaw, 2003). Presently more than 200 optically stimulated luminescence (OSL) ages are available for aeolian sediments from South Africa, Botswana, Namibia, Zimbabwe and Zambia that elucidate changes in desert conditions and dune activity in the Mega Kalahari. This has given good insights into the dynamism of the Kalahari Desert and led to a further movement away from Lancaster's model to a more complex model of episodic aeolian activity at regional levels occurring over different time periods (Thomas and Shaw, 2003). These studies have led to tentative differentiation between aeolian activity in the core areas of the Kalahari, (e.g. the Northern Cape of South Africa and southwest Botswana), and the marginal areas such as western Zambia, where the aeolian activity is less frequent and less extensive. Distinctions between core and marginal areas are largely thought to be a function of the timing and magnitude of precipitation penetration into the region. As such the aeolian sedimentary record can be used infer to past arid climatic conditions (Thomas and Shaw, 2003) and the amplitude of ITCZ penetration (Stokes et al., 1997a).

2.2 Limitations of the existing OSL chronology

There are two drawbacks with the current OSL chronology: 1) the issue of differentiation between episodic and continual sedimentation and 2) the limited depth of the total aeolian record that has been sampled. In the Kalahari, the aeolian sediment accumulations attain thicknesses ranging from a few metres to tens of metres, and luminescence dates on samples up to 6.5 m below the surface (e.g. Stokes et al. 1997a) have been obtained. In most locations, these aeolian deposits are notable for their limited internal stratigraphy but even without clear stratigraphic evidence the frequent assumption in published chronologies is that the age data represents episodic rather than continuous sedimentation. However, no gaps in the overall OSL chronology are readily apparent in which quiescent periods or periods when no aeolian sedimentation occurred can be easily inferred. Singhvi & Wintle (1999), using cumulative probability plots of the OSL ages of Stokes et al. (1997a), showed episodes of more intense sand accumulation over the last 150 ka whilst interpretation of contiguous aeolian and lacustrine records at specific locations also suggests hiatuses in aeolian accumulation (Thomas et al., 2003).

What is also clear from the dataset of luminescence ages for the Kalahari, and exemplified by Singhvi & Wintle (1999; Fig. 13.3), is the paucity of luminescence ages beyond 50 ka. The 6.5 m exposure in a linear dune in Zimbabwe provides the longest site chronology (Stokes et al*.,* 1997a). This chronological limit could be due to aeolian activity in the Kalahari increasing in intensity and extent over the last 100,000 years. However the cyclical nature of Quaternary climates in terms of glacial-interglacial transitions makes it seem unlikely that enhanced aridity and Kalahari expansion occurred only during the latter part of the last glacial cycle. Also, from insolation reconstructions, Partridge et al. (1997) have reported the existence of drier phases, during oxygen isotope Stage 6 and earlier. Aridity beyond the last glacial-interglacial cycle awaits rigorous testing at a regional scale. It appears far more likely that the dataset of luminescence ages and the inferred episodes of aridity, in part reflects the sampling strategy and are additionally affected by effects of sediment recycling/burial.

2.3 OSL Sampling Strategies

OSL dating relies on the exposure of sand grains to daylight to reset the luminescence clock. A near complete resetting of the OSL signal down to a residual level can occur in less than one minute's exposure to daylight (see Aitken 1998). In respect to palaeoenvironmental research on aeolian sediments in the Kalahari, the high sensitivity of the method to daylight exposure ensures that all OSL signal in sand grains should be reduced to their minimal residual level prior to burial. Therefore, derived OSL ages should be true burial ages with none of the OSL signal being derived from previous sedimentary cycles. On the other hand, such a high sensitivity also implies that local reworking events (such as caused by local droughts or removal of vegetation by fire) are potentially as effective in resetting the OSL signal as climate-induced dune building events. To avoid any confusion arising from resetting by local events leading to misinterpretation of complex regional palaeoenvironmental changes, a large OSL data set with good spatial coverage is needed. Such a high density sampling approach has been adopted (e.g. Stokes et al 1997a; Lawson and Thomas 2002). Much of the luminescence data set, which forms the core of the chronology for the Kalahari, has been derived from pits dug in the crestal regions of dunes, a strategy that ruled out depositional processes other than aeolian. As the unconsolidated sands of the Kalahari preclude the digging of pits of greater than 2 m, superficial sediments are over-represented in the data set. Secondly, the sampling of dune crests also implies that places in the landscape which are most susceptible to aeolian reactivation are the ones that have been sampled.

Thus, sample site selection is extremely critical and needs a careful balance between avoiding areas in which the OSL signal is reset by sediment recycling on decadal time scales due to drought, and areas that capture signatures of major aridity events. Two possible sampling strategies exist for extending the chronology back further in time. The first one is to sample the presently relict marginal areas that should have been active during major, Mega Kalahari wide aridity events, e.g. O'Connor and Thomas (1999). An alternative is to utilise more of the sedimentary record rather than the geomorphic record and obtain sediment from deep exposures which are unlikely to have suffered multiple sediment recycling phases.

The aims of the present study are three fold. First new OSL data from an extensive exposure of aeolian sandsheet sediments at the Mamatwan maganese mine in the SW Kalahari is presented. This record is then compared with previously published records of the SW Kalahari aeolian deposition. Finally, the new data are combined with the rest of the SW Kalahari OSL dataset to examine how different aeolian depositional styles have different potentials in preserving long-term environmental records.

3. Study Sites

3.1 Mamatwan (27^{o} 22' S 22^{o} 58' E)

The Mamatwan open cast mine is approximately 20 km south-west of Hotazel in Northern Cape Province, South Africa. It is situated in a topographical low within the Molopo sub-basin of the Kalahari and bounded in part by the Kuruman and Korannaberg hills (Fig. 1). The mining company Samancor extract *ca.* 300,000 tonnes of manganese per annum from the mine and in doing this have had to remove between 40-50 m of Kalahari Group as overburden. The manganese ore is part of the 2300 Ma Protozoic deposits of the Voelwater Formation and the Kalahari Group sediments lie unconformably over it. The mine is divided into 3 benches (Fig. 2) and the stratigraphy is described below based on field observations and the descriptions of Williams (1993) and Bootsman (1998).

Unit I: Red Clay
At the base of the lowest bench and locally absent is a red (2.5YR 4/4) clay unit which according to borehole data thickens westward ranging from between 0.5-27 m. This is interpreted as a lacustrine deposit formed when the proto-Molopo river (the major pre-Kalahari river in this region) was affected by the uplift along the Grique-Transval axis. This unit was not visible in the Mamatwan exposures at the time of sampling.

Unit II: Managanese Palaeosol
This 2 m thick unit is composed of maganese nodules which increase in angularity down unit and are enclosed in a matrix of pale pink calcrete veins and calc-arenite. It is interpreted as a palaeo-weathered horizon or palaeosol modified later by calcrete growth and may be the lateral equivalent of unit I.

Unit III: Calcareous Breccia
This 8-10 m thick unit is dominated by a low density pale pink coloured clay-silt sized calcareous material with occasional small rounded ironstone and manganese pebbles in the lower 2 m. Clasts exhibit concentric onion ring alteration whilst the low density is due to the high sepiolite clay content. Its occurrence directly on Unit I in places led Bootsman (1998) to suggest that this unit represents distal-end alluvial fan deposits which were subsequently calcretised under fluctuating water-table levels and under climatic conditions much wetter than present.

Unit IV: Channel Calcrete

This unit has a sharp erosional contact with the underlying breccia, has a variable thickness (1-3 m), and grades up into Unit V. It is composed of medium to large, rounded, banded ironstone and manganese pebble and cobble sized clasts which have been subsequently calcretised. The unit is interpreted as a channel lag deposit with thinner parts of the unit representing overbank deposits.

Unit V: Calcrete
A 8-10 m thick unit comprising of fine to medium sized quartz grains incorporated into a calc-arenite which is

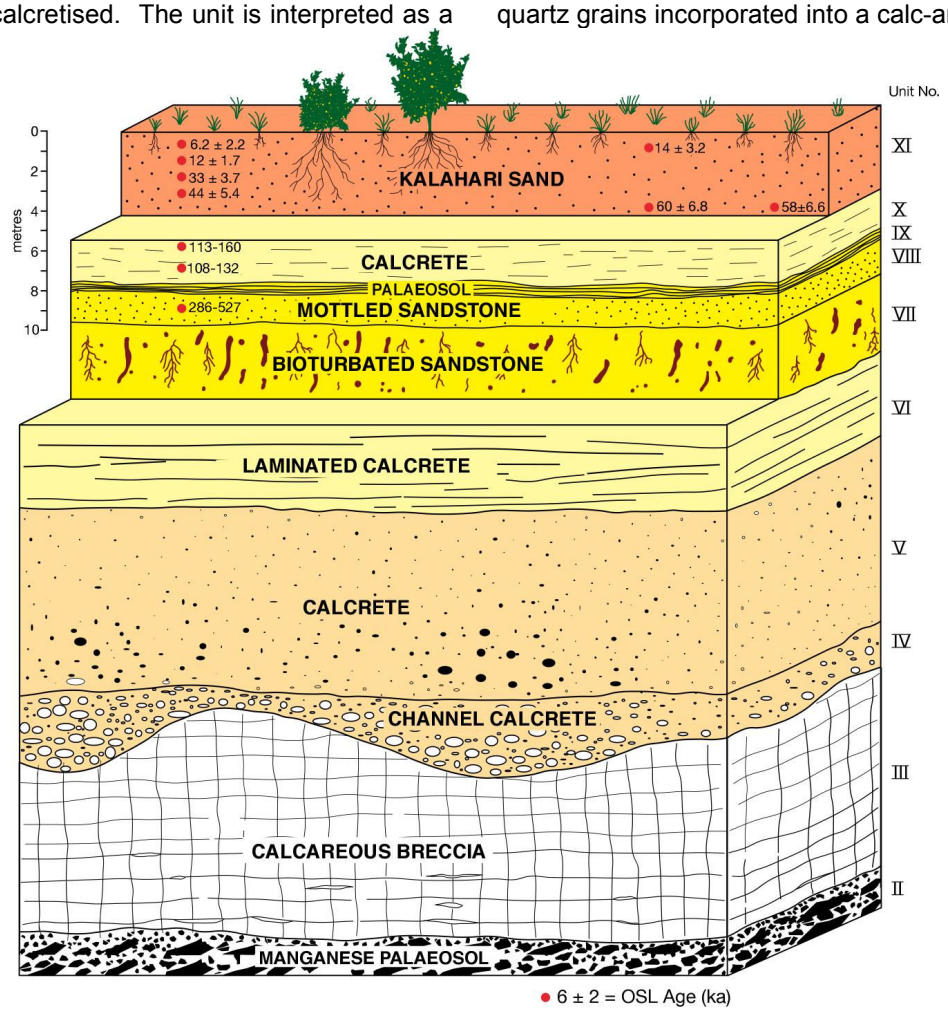

Figure 2. Stratigraphy and OSL age estimates of the Mamatwan mine, Hotazel, South Africa.

sub-horizontally laminated in places. This unit grades upwards to Unit VI.

Unit VI: Laminated Calcrete
A 4 m thick unit of calcrete with numerous horizontal laminations of crystalline calcrete within a calc-arenite matrix.

Unit VII: Bioturbated Sandstone
Up to 5 m in thickness, this unit is a fine grained orange sandstone in which former rootlets have been replaced by pale pink/white calcrete.

Unit VIII: Mottled sandstone
This unit is up to 1.5 m thick and comprises a fine to medium grained sandstone dominated by rounded to well-rounded fine quartz sand with minor amounts of heavy and opaque minerals. Micromorphological analysis by D. Nash at Brighton University shows the sediment to be moderately to well-cemented with a variable pore space of around 7%. It appears that the cement initially developed as an iron-rich coating in association with clay minerals giving many grains a 'halo' of iron oxide. Iron staining of later cementing (a mixture of calcium carbonate and silica) suggest reasonable amounts of iron within the precipitating solution. There is no clear pattern to the distribution of silica and calcium carbonate within the cement suggesting that there may have been multiple phases of cement precipitation and periodic diagenetic alteration of previously precipitated cements. The matrix is mottled by orange-red stained patches of uncemented red sand which can have diameters between 0.5 - 2 cm.

Unit IX: Palaeosol
This is a 0.5 m thick brown/orange unit containing horizontal laminates as well as contorted bedding, interpreted as either a palaeosol or an iron pan resulting from water-table fluctuations.

Unit X: Calcrete
This units comprises a blocky and massive calcrete, approximately 2 m thick with fine to medium grains incorporated into it. It grades upwards into a fine powdery/nodular calcrete which in turns grades into Unit XI. Some red sand inclusions and manganese nodules occur within the block elements of the calcrete.

Unit XI: Kalahari Sand
This unit is up to 4 m thick and comprises loosely compacted medium grained orange-red rubified quartz rich sand with carbonate cementation increasing with depth. The particle size distribution of this sand is typical of the aeolian facies of the Kalahari sands (Fig. 3). Dunes are not widely present in this eastern part of the SW Kalahari and this unit

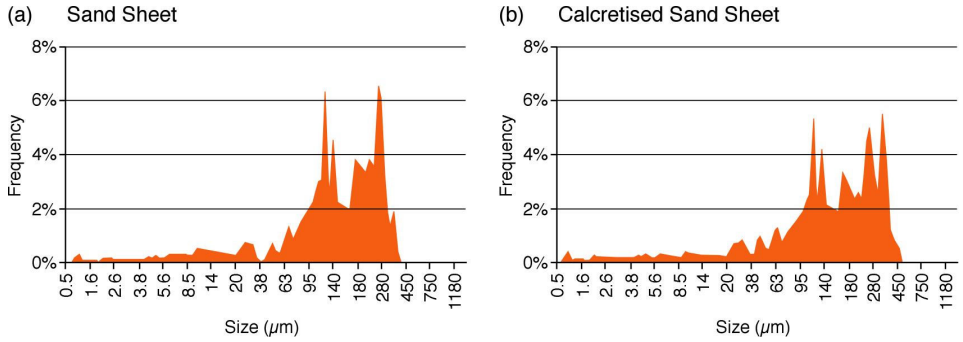

Figure 3. Particle size distributions of (a) Kalahari sand from Unit XI at Mamatwan (b) calcretised sand from Unit X. All measurements carried out on a Cilas laser diffraction system.

represents an aeolian sand-sheet possibly derived by reworking of earlier sandy deposits.

The sedimentary succession at the Mamatwan mine indicate a range of depositional environments (ranging from fluvial and lacustrine in the lower units to aeolian in the upper units) suggesting significant environmental changes. Evidence of mottling and cementation could imply a history of water table fluctuations and/or seepage of calcium carbonate enriched groundwater during the past. In terms of the Kalahari sand, the site is well placed, in that not only is a significant thickness of sediment revealed but also the area is marginal to the core Kalahari Desert so potentially it will have seen significant aeolian sediment deposition only during major aridity events.

In order to put a chronology to some of these events the Mamatwan mine was sampled for luminescence dating. A total of 10 samples were taken including 7 from Unit XI, 2 from Unit X and one from unit IX. Duplicate samples from similar stratigraphic positions and depths but at different localities within the Mine were taken to act as a semi-independent check on the chronology.

3.2 Linear Dunes sites

For comparative purposes a number of new linear dune sites from the SW Kalahari were sampled (Fig. 1). These sites were selected to fill in spatial gaps in the existing luminescence chronology of the SW Kalahari (Stokes et al. 1997a; 1997b; Thomas et al. 1997). Site CT96/10 (27° 15' S, 20° 47' E) located 150 km north of Upington, is one of many linear dunes cut through by a new tar road to the Kgadigadi Transfrontier Park. From this site two samples were collected for luminescence dating. Site Kal98/2 dunes (26° 45' S, 20° 03' E) was located in the Mier District of South Africa within a region of presently partially vegetated linear. A pit in the crest of one dune provided two samples for luminescence dating. Finally site Kal98/3 (26° 55' S, 22° 45' E), where a single sample was collected for luminescence dating, was located on the summit of a 30 m+ linear dune parallel to the Kuruman valley.

4. Luminescence Dating

4.1 Linear dune and sandsheet samples

4.1.1 Experimental Details

Extraction procedures to obtain clean quartz fractions from the sand from Unit XI at Mamatwan and from the linear dunes sites, followed Bateman and Catt (1996). All samples were measured at the Sheffield Centre for International Drylands Research luminescence laboratory using an upgraded Risø TL-DA-12 reader. Optical stimulation was provided by a 150 W halogen

lamp filtered with GG-420 and SWP interference filters and the resultant luminescence was measured through a 5 mm thick Hoya U-340 filter.

The palaeodose (D_e) for each sample were determined using the single aliquot additive dose protocol (SAAD) originally outlined by Duller (1994) for feldspars (for details see Aitken, 1998) and successfully applied to quartz by Murray *et al.* (1997). Between 6 and 12 replicates per sample, were measured using a preheat of 220 ^{o}C for 120 s and stimulation for 0.2 s at 50 ^{o}C. Data for correcting the effects of repeated preheating and measurement was collected on 3 separate aliquots. The additive dose strategy aimed to give a maximum laboratory dose approximately 5 times the estimated palaeodose for each sample, and the growth curve was characterised by seven additive dose points (Fig. 4). An additional 2 dose points were measured at the maximum dose in order to check that the correction procedure was working appropriately. All samples gave corrected OSL intensities that were internally consistent, showing this was the case. Data was analysed using Rainer Grün's APP-SIM program. Finally a single SAAD palaeodose was calculated from the weighted mean (according to variance) for all aliquots measured for each sample (Table 1).

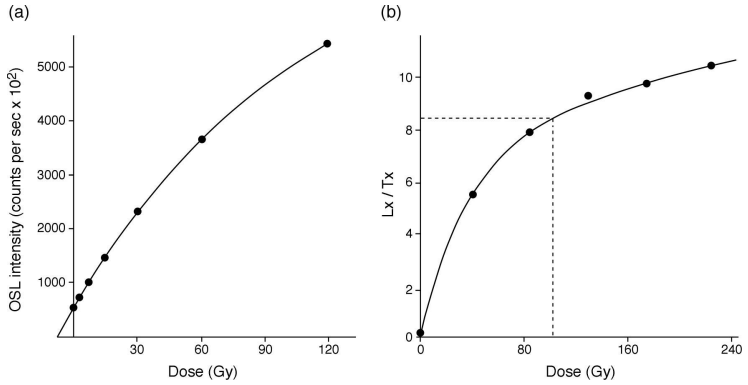

Figure 4. (a) SAAD growth curve for sample Shfd990074 (b) OSL decay curve and SAR growth curve for samples Shfd99077.

Table 1: Sample details and OSL data for Mamatwan mine, and linear dune site SW Kalahari, South Africa

Sample	Lab Code	Depth (m)	Stratigraphy	Palaeodose (De) (Gy) SAAD	Palaeodose (De) (Gy) SAR	Dose Rate (μGy/ka)		Age (ka)
Mamatwan Mine, Hotazel, 27° 22' S 22° 58' E								
Kal98/4/1	Shfd99073	0.50	Top of sand	6.26 ± 2.2	-	1009 ± 87 †		**6.2 ± 2.2**
Kal98/5/1	Shfd99080	0.70	Top of sand	13.6 ± 3	-	1004 ± 87 †		**14 ± 3.2**
Kal98/4/2	Shfd99074	1.00	Sand	12.3 ± 1.4	-	993 ± 87 †		**12 ± 1.7**
Kal98/4/3	Shfd99075	1.60	Sand	32.2 ± 2.3	-	985 ± 88 †		**33 ± 3.7**
Kal98/4/4	Shfd99076	2.60	Base of sand	48.4 ± 3.8		1109 ± 106 †		**44 ± 5.4**
CT96/11/1	Shfd97030	3.00	Base of sand	48.2 ± 1.8	-	806 ± 86 †		**60 ± 6.8**
CT96/11/2	Shfd97031	3.00	Base of sand	46.8 ± 1.6	-	802 ± 86 †		**58 ± 6.6**
Kal98/4/5	Shfd99077	3.20	Calcrete/Sand	-	120 ± 15	1061 ± 36 ‡	752 ± 28 ‡	**113 ± 15 – 160 ± 20**
Kal98/4/6	Shfd99078	5.90	Calcrete	-	340 ± 73	3149 ± 123 ‡	2569 ± 108 ‡	**108 ± 24 – 132 ± 29**
Kal98/4/7	Shfd99079	6.80	Sandstone	-	388 ± 60	1359 ± 118 †	736 ± 30 ‡	**286 ± 51 – 527 ± 84**
Grootdrink, Kuruman Valley, 26° 55' S 22° 45' E								
Kal98/3/1	Shfd00068	0.60	Linear Dune	-	5.54 ± 0.10	817 ± 0.078 †		**6.8 ± 0.7**
Mier Farm, 26° 45' S 20° 03' E								
Kal98/2/1	Shfd98065	0.50	Linear Dune	16.5 ± 2.0	-	2398 ± 203 †		**6.9 ± 1.0**
Kal98/2/2	Shfd98066	1.40	Linear Dune	21.8 ± 1.6	-	2373 ± 203 †		**9.2 ± 1.0**
North of Upington, 27° 15' S 20° 47' E								
CT96/10/1	Shfd97027	2.10	Linear Dune	15.2 ± 0.6	14.21 ± 1.56	1154 ± 46 †		**13 ± 0.7**
CT96/10/2	Shfd97028	1.00	Linear Dune	4.60 ± 0.5		1190 ± 47 †		**3.9 ± 0.2**

† dose rate based on field measurements using portable gamma-spectrometer
‡ dose rate based on ICP results on sample which had undergone stringent acid washing to remove post-depositional carbonate material.
* Age calculated using the SAAD derived palaeodose

Recently some doubt has arisen over the use of the SAAD protocol on quartz due to its absence of correction for laboratory induced sensitivity changes (e.g. Stokes et al., 2000). Such sensitivity changes appear to partly relate to the extent of bleaching of the sample prior to burial, its antiquity and the intrinsic OSL characteristics of the quartz (dependant on geological source and environmental history). However the results presented by Murray et al. (1997) and Stokes et al. (2000) show that for well-bleached desert quartz, as opposed for example to fluvial derived quartz, problems in estimating D_e using the SAAD protocol were far less pronounced. Additionally, the use of a second set of aliquots, as adopted above, to characterise the pre-heat-OSL decay form does provide much more reliable SAAD D_e estimates for quartz (Stokes et al. 2000). In order to further check the validity of the SAAD data from the present set of samples, one sample (Shfd97027) was also run using the single aliquot regenerative (SAR) protocol (Murray and Wintle 2000) which corrects for possible laboratory induced sensitivity changes s (see below for details). Both the SAAD and SAR results were concordant within errors, implying that in the present batch of samples sensitivity changes did not occur and that the SAAD results could be relied upon. A similar comparison of SAAD and SAR on Kalahari sand from northern Botswana (Thomas et al., 2003) also showed that a majority of samples gave concordant results. Such results gives confidence that the SAAD results presented here, and those previously published and used in Section 5.3 (e.g. Lawson and Thomas 2002) can be relied upon.

4.1.2 Dose Rates

Dose rates were calculated for the sand-sheet and linear dune samples based on measurements with a field multi-channel EG&G Micro-Nomad portable gamma spectrometer (PGS) with corrections for attenuation due to grain size, quartz density and water content. Palaeo-moisture values were assumed to have been similar to the present day although errors of $\pm$ 2% were adopted to take into account past fluctuations. The cosmic dose contribution was calculated following the algorithm set out in Prescott and Hutton (1994). All these samples were assumed to have been in radioactive equilibrium and the concordance of inductively coupled plasma (ICP) and PGS data for sample Shfd99076 supports this assumption (Table 2).

4.2 Calcrete and sandstone samples

Given that one of the limitations of the Kalahari OSL dataset outlined above is the paucity of ages beyond 50 ka, we were keen to see if we could utilise as much of the extensive Mamatwan Kalahari Group sequence as possible to extend the record. Units VII-X may represent the lower elements of the Kalahari sand in which alteration has progressively occurred. If reliable depositional ages could be obtained from quartz grains within these units there is the potential to extend back the aeolian aridity chronology for the SW Kalahari. In order to establish whether Units VII-X were of aeolian origin, particle size analysis on the sand fraction from the uppermost calcrete sample and from a sample from Unit XI was conducted using a Cilas laser defraction system. Figure 3 shows that both samples display almost identical bimodal distributions that are consistent with many Kalahari aeolian sediments (Livingstone et al., 1999). It is therefore assumed that these units are lower elements of Kalahari sand and are of an aeolian origin.

The application of luminescence dating to calcretised samples such as those sampled from Units VIII-X at Mamatwan is not optimal nor straightforward. Measurement of the D_e for well bleached aeolian sands should only be problematic if the OSL is in saturation. Otherwise the measured D_e's should relate to burial age. However calculation of the annual dose is complex where post-depositional alteration has caused the concentration or leaching of naturally occurring radionuclides, causing the dose rate to change through time. Micromorphological evidences of multiple phases of cementation, together with a lack of knowledge of the timing and amplitude of such alterations makes it difficult to model such dose rate changes. Due to assumptions about dose rate fluctuations through time, the procedure outlined below provides only preliminary age estimate ranges for the calcrete/sandstone units which future work can improve upon.

4.2.1 Experimental Details

The calcrete and sandstone samples were prepared in the same way as outlined in Section 4.1.1 except they underwent an additional pre-treatment involving gentle crushing down to a fine gravel/coarse sand size and steeping in concentrated HCl (35-38%) to remove any carbonate based cementation material. The single aliquot regeneration (SAR) protocol of Murray and Wintle (2000), was applied on account of difficulties in producing well characterised SAAD growth curves for meaningful D_e extrapolation. With the SAR protocol, an OSL response to a test dose was used to correct for sensitivity changes caused by repeated preheating and measurement on the same aliquot.

Table 2 Selected data used for the calculation of dose rates for the Mamatwan mine site as measured by portable gamma spectrometry (PGS) and inductively coupled plasma (ICP) spectroscopy.

Sample	Lab Code	Depth	Stratigraphy	PGS Data (in situ)			ICP data (no HCl treatment)			ICP data (HCl treatment)		
		(m)		U (ppm)	Th (ppm)	K (%)	U (ppm)	Th (ppm)	K (%)	U (ppm)	Th (ppm)	K (%)
Kal98/4/1	Shfd99073	0.50	Top of sand	0.6	2.7	0.4				0.6	2.3	0.3
Kal98/4/4	Shfd99076	2.60	Base of sand	0.6	2.9	0.6				0.6	2.8	0.4
Kal98/4/5	Shfd99077	3.20	Calcrete/Sand	0.9	2.9	0.6	1.3	2.4	0.4	0.6	2.2	0.3
Kal98/4/6	Shfd99078	5.90	Calcrete	1.0	3.4	0.7	3.4	8.4	1.6	1.9	8.1	1.41
Kal98/4/7	Shfd99079	6.80	Sandstone	0.9	3.9	0.8				0.7	2.5	0.28

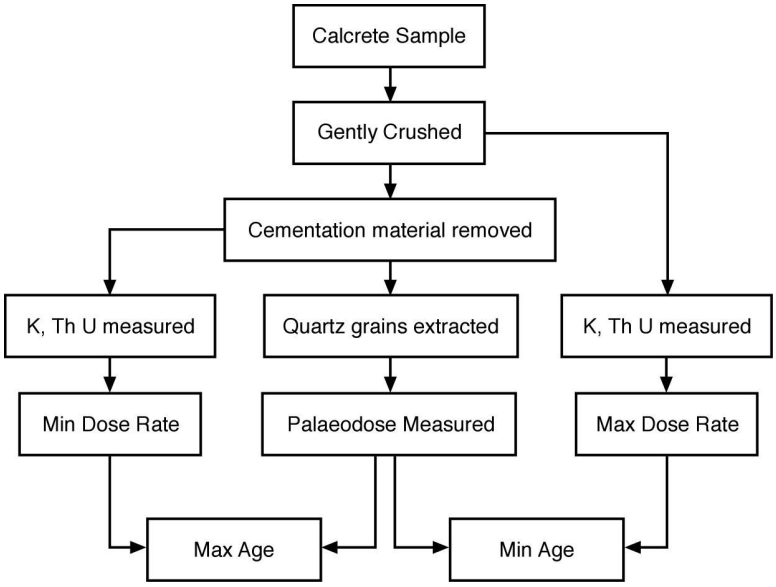

Figure 5. Schematic diagram showing the sample preparation and measurement protocol used to derive age range estimates for the calcretised samples.

A seven point regeneration strategy was adopted with five dose points used for bracketing the palaeodose, a sixth zero dose and a seventh repeat of the first dose point (Fig. 4). All measurements used a preheat of 260 ^{o}C for 10 s with OSL measurements carried out at 125 ^{o}C for 100 s. The ratio between the first and seventh points was used to check that the sensitivity correction procedure was working. In all cases this ratio fell within 1.0 $\pm$ 0.1. All the data was analysed using Duller's ANALYST program. Twelve replicates per sample were carried out with final D_e values derived from a weighted (by variance) mean.

4.2.2 Dose Rates

Exact dose rates for the samples from Units VIII and X at Mamatwan are impossible to derive as the timing and duration of calcretisation/cementation and hence the change of dose rate is unknown. Singhvi et al. (1996) reported a methodology to date pedogenic carbonates by assuming the age of the quartz contained within the carbonate nodules was the same as found outside. From this they derived equation 1 which can be solved to get the age of carbonate nodule formation.

Equation (1)
$$t_c = \frac{Q_s - Q_c}{D_{\beta.s} - D_{\beta.c}}$$

where Q is the equivalent dose either for s (sand) or c (calcrete) and D is the dose rate either for sand or calcrete. Simple dosimetric considerations indicate that only the beta dose is affected by such nodule development.

Such an approach is not valid for the Mamatwan samples as they form massive, rather than nodular, beds and the assumption that over- and under-lying sand beds are of equivalent age is impossible to justify. However, it is possible to derive minimum and maximum age estimates if a simple model of alteration is assumed. Two extreme cases provide upper and lower bounds. These are 1), that the calcretisation occurred soon after sand emplacement and 2), that it was a very recent

development. Equations 2a and 2b can be used to calculate the minimum and maximum ages associated with these two extreme scenarios.

Equation (2a) $$t_{min} = \frac{Q_s}{D_c}$$

Equation (2b) $$t_{max} = \frac{Q_s}{D_s}$$

Where t_{max} is the maximum age estimate (late arrival of carbonate), t_{min} is the minimum age estimate (early arrival of carbonate), Q_s is the palaeodose received by the quartz grains since burial, D_s is the dose rate derived from HCl acid-washed sand and D_c is the dose rate from the calcretised sand. In order for this simple alteration model and procedure to be valid for the calculation of 'true' minimum and maximum dose rates, a number of assumptions on the manner of how alteration affected the dose rate, are needed.

One assumption is that the two measured dose rates are accurate. Conversion from elemental concentrations as determined by ICP to dose rates assumes that the Uranium (U) and Thorium (Th) decay chains are and have always been in equilibrium. Whilst disequilibrium in the Th chain is rare in naturally occurring sediments, it is common for the U chain (Olley et al., 1996). Given the complex history of post-depositional alteration of the sediments, with both cementation and iron staining (with likely co-precipitation of U), the assumption of equilibrium for the calcrete/sandstone samples is unlikely to hold true. As ICP measures parent isotopes and PGS measures short-lived daughters (^{214}bismuth and ^{208}thallium for U and Th respectively) further down the decay chain, if disequilibrium exists then a significant difference between the two techniques is to be expected. When ICP and PGS data from two of the untreated calcrete samples (Shfd99077 and Shfd99078) are compared differences are apparent with the PGS data for U being 30% and 70% lower (Table 2). Lower U values indicate either a net loss of daughter-isotopes in the U chain, e.g. by radon loss, or excess in parent. The effect of the former has potentially more of an impact on dose rates as only 25% of U contribution to annual dose is derived from the pre-radon part of the decay chain (Olley et al., 1996). However, as the U contribution to the total dose rate is relatively small (~15%) and reported U disequilibrium is generally less the 50% (Olley et al., 1996) it is contended that the effects of disequilibrium are unlikely to significantly alter the age ranges calculated which themselves include uncertainties of between 13-22%.

Another assumption made is that the HCl treatment reduces the samples back to their pre-cemented state. Micromorphological analysis of Unit VIII showed that a minor component of silica had been added which concentrated HCl would not have removed. Additionally whilst the acid treatment would have removed amorphous iron oxide coatings it would not have removed older crystalline iron coatings. Elemental concentrations after HCl treatment of sand from the base of Unit XI (Shfd99076) and the calcrete sampled 60 cm beneath it (Shfd99077) shows the HCl treatment to be successfully reducing the calcrete sample back to its unaltered state (Table 2). This also seems to be the case for sample Shfd99079 but not for sample Shfd99078 which shows persisting high levels of U, Th and K compared to the sand from Unit XI.

The dose rates used in the final age calculations for these samples were based on concentrations as determined by sodium peroxide fusion digestions followed by measurement by ICP-mass spectrometry for U and Th and ICP-emission spectroscopy for K at XRAL laboratories, Canada. These were converted to dose rates using the values in Aitken (1985, p.67). The minimum dose rate was calculated from untreated sub-samples whilst the maximum dose rate from sub-samples which had been pre-treated with HCl to remove carbonate material. An exception to this was sample Shfd99079 where there was insufficient material so the maximum dose rate was based on PGS data. The cosmic dose contribution was calculated following the algorithm set out in Prescott and Hutton (1994). Overall in view of the cosmic ray dose and significant contribution by K, it is considered that any effects arising out of disequilibrium of the U –series are likely to be small.

4.3 Ages

Table 1 and Figures 1 and 2 provide the ages for the Mamatwan mine and linear dune sites. For calcrete/sandstone samples the true age for the calcrete/sandstone samples should fall within the calculated age ranges. The sampling strategy for Unit XI at Mamatwan was such that samples for similar stratigraphic positions but from different locations in the quarry could be used as checks. These pairs (Shfd99080-Shfd99074 and Shfd97030-Shfd97031) show good age agreement (Fig. 2). Similarly at Mamatwan the age estimates increased with depth and show a jump in age associated with the stratigraphic change from Unit VIII to Unit X.

5. Discussion

5.1 Mamatwan

If all the assumptions for the calcrete dates are valid, then Units VIII-XI represent deposition at least during the last *ca.* 300 ka. Although OSL samples deeper than 11 m were not collected, the total of 40 m of

exposed sediments at the Mamatwan site has the potential for developing a long terrestrial record of environmental change, possibly dating beyond the Quaternary. Further work is ongoing to extend this chronology and refine methods of OSL dating calcretised aeolian sediments.

Excluding the least reliable age range (Shfd99079), the other nine ages from Mamatwan fall into 3 groupings (Fig. 6); the last interglacial, 35-60 ka and *ca.* 6-14 ka. In contrast to previous work on the linear dunefields of the SW Kalahari, no Last Glacial Maximum (LGM) ages were determined. This in itself is interesting as either this period is missing from the record at this location, or sediments of this age were missed during sampling. Given the lack of structure in the Kalahari Sand at Mamatwan, a feature common throughout the Kalahari, it is not possible to rule out a temporal hiatus in deposition.

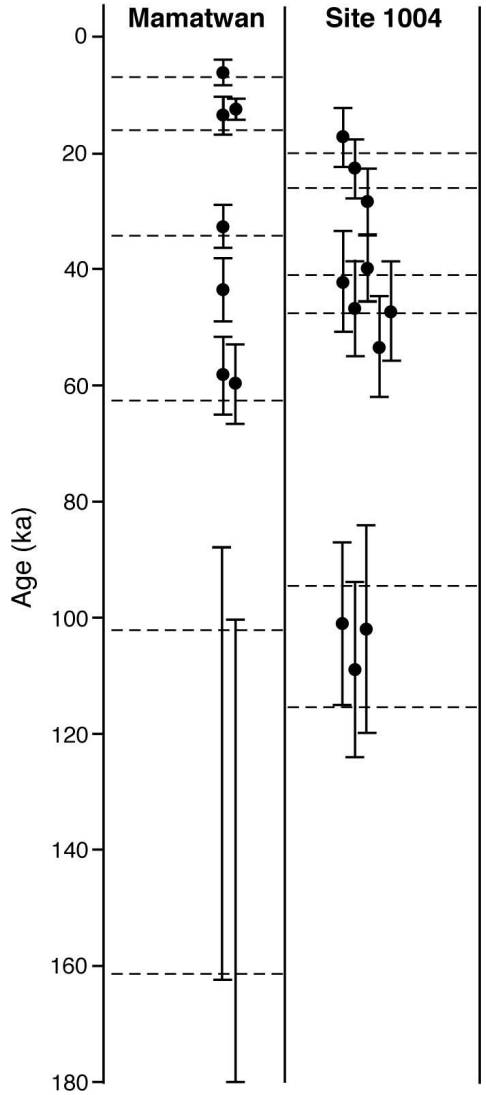

Figure 6. Comparison of the Mamatwan OSL chronology to that of the master chronology from site 1004 (Stokes et al. 1997a).

If the LGM was missed during sampling, then only a maximum of 0.6 m of LGM sediments (the distance between samples Kal 98/4/3 and Kal 98 4/2) exist at Mamatwan, although reworking of other LGM sediments by the final (13-6 ka) phase of aeolian activity cannot be ruled out

When the Mamatwan data are compared to the longest reported record of Stokes et al. (1997a) there are similarities, in identifying aeolian phases

both 40-50 ka and in the period 115-95 ka (Fig. 6). In the most recent parts of the record there are, however, dissimilarities. Site 1004 shows aeolian activity during the Last Glacial Maximum, while Mamatwan records sand deposition in the Lateglacial-early Holocene period. Site 1004 is considerably further NE of Mamatwan and presently experiences much higher annual rainfall due to the precipitation gradient over the Kalahari. Thus the differences in aeolian activity described above may be because one is comparing deposition in different sub-regions of the Kalahari as shown by Thomas and Shaw (2003). It may also be a consequence of comparing data from a sand-sheet location with that from a linear dune, both of which will have different environmental controls and different sensitivities to changes in aridity. This is discussed further in section 5.3.

5.2 Linear Dune Sites

The new dates from the 3 linear dune sites in the region around Mamatwan are significant for two reasons. Firstly none of the ages date to the time around the Last Glacial maximum or older. This is despite linear dunes of LGM age being reported elsewhere in this region (e.g. Thomas et al., 1997). The new dates suggest that the enhanced linear dune activity during the LGM in the SW Kalahari was on a sub-regional scale resetting all the OSL 'clocks' but this was then followed by more local reworking/recycling of linear dune sediments through the Lateglacial to Mid Holocene.

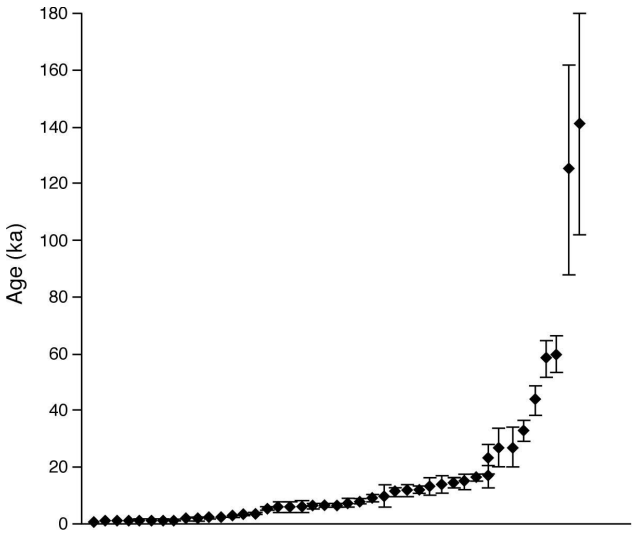

Figure 7. Compilation of the OSL ages for the SW Kalahari from Stokes et al., 1997a; Thomas et al., 1997; Lawson, 1998; Lawson and Thomas, 2002 and this paper. Ages are plotted in ranked order from youngest to oldest.

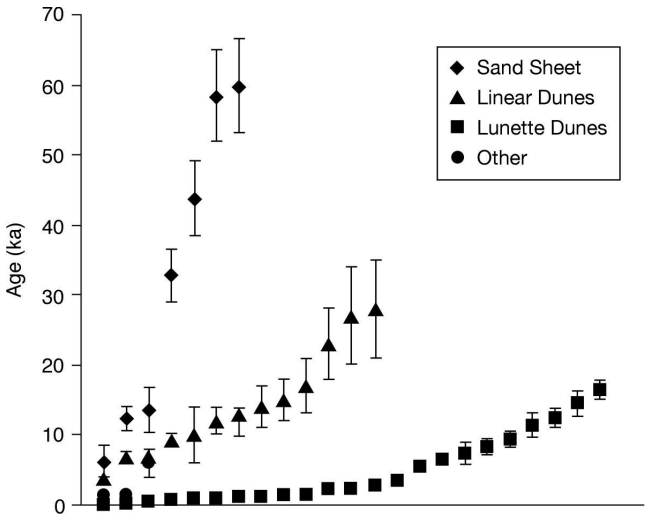

Figure 8. Compilation of the OSL ages for the SW Kalahari categorised by depositional style. Data from Stokes et al., 1997a; Thomas et al., 1997; Lawson, 1998; Lawson and Thomas, 2002 and this paper. Ages are plotted in ranked order from youngest to oldest.

Secondly the new linear dune OSL ages pick out a phase of activity between 4-13 ka which is comparable to the most recent found at Mamatwan. Thus major restructuring of linear dunes and sediment recycling did not occur during this timeframe, as both the linear dune and sand-sheet record at Mamatwan are concordant.

5.3 Aeolian styles and the Palaeorecord

Using the new data presented above and combining it with previously published luminescence ages for the SW Kalahari (Stokes et al., 1997a; 1997b, Thomas et al., 1997; Lawson 1998) it becomes apparent that periods when aeolian sand was not being deposited somewhere in the SW Kalahari during the last 50 ka are very hard to identify (Fig. 7). Small gaps are probably an artefact of sampling rather than inferring periods of increased humidity. However, if the same data are plotted according to the type of aeolian deposit from which they were derived, (Fig. 8), it becomes clear that different landforms were active and/or have preserved evidence over different time scales. The Mamatwan sand-sheet shows the longest record, from the last interglacial period and beyond. The linear dune record seems to be dominated by dates from the LGM through to the early Holocene whereas lunette dunes tend to date between the Lateglacial period right through to almost the present day. What is clear is that the Lateglacial period was a period of activity in all types of aeolian system in the region, providing the best preserved sedimentary record for the SW Kalahari.

As Mamatwan is showing aeolian deposition prior to the LGM it is hard to imagine that the core SW Kalahari Desert was not also active to some degree at this time. Without this, Mamatwan would have remained sediment starved, as the net transfer of aeolian sediment from the NW relies of movement along the linear dunes. If this is valid, then the data illustrates that the linear and possible lunette record has been reset by the intensity of the activity from the LGM onwards.

6. Conclusions

It is possible to extend the palaeoenvironmental record of the Mega Kalahari back beyond the LGM by looking for sites that are peripheral to core desert activity and/or multiple periods of sediment recycling. The position of Mamatwan on the margins of the SW Kalahari in a sedimentary sump and with OSL ages spanning at least the last 300 ka exemplifies this well.

It is clear that different aeolian depositional styles have different sensitivities to climate and therefore will have different abilities to respond to, record, and store climate changes. Lunette dunes seem to react more readily to changes compared to linear dunes although both suffer from sediment recycling preventing longer-term preservation of Quaternary records. Sand-sheets may not suffer from this to the same extent but further work is needed to understand sediment supply to them and to make it possible to identify hiatus(es). The sampling of different geomorphic features will lead not only to a complex record but will limit, in some cases, the temporal extent of that record. This does have positive attributes as sampling a range of depositional

styles will give key information to help in understanding the intensity of changes and the impact of non-climatic variables (e.g. vegetation) in past environments, although such an understanding relies upon a good understanding of contemporary processes.

7. Acknowledgements

The authors wish to acknowledge the support of The Sheffield Centre for International Drylands Research and the Sheffield University Research Fund which supported the fieldwork for this work. AKS undertook the work on dating calcretes whilst on a Leverhulme fellowship at Sheffield University. Thanks are also extended to David Nash (Brighton University) for his micromorphology work and for the comments of John Magee and Geoff Duller at the refereeing stage, which have considerably improved the paper. This is a publication as part of the IGCP-413 programme *' Understanding Future Dryland Environmental Changes from Past'*.

7. References

Aitken, M. 1985. Thermoluminescence Dating. Academic Press, London 359pp.

Aitken, M. 1998. An Introduction to Optical Dating. Oxford University Press, Oxford, 267pp.

Bateman, M.D. and Catt, J.A. 1996. An absolute chronology for the raised beach deposits at Sewerby, E. Yorkshire, UK. Journal of Quaternary Science 11, 389-395.

Bootsman, K.S. 1998. The evolution of the Molopo drainage. Unpublished PhD thesis, University of the Witwatersrand, South Africa, 261p.

Butzer, .K.W., Struckenrath, R., Bruzewicz, A.J. and Helgren, D.M. 1978. Late Cenozoic paleoclimates of the Gaap Escarpment, Kalahari margin, South Africa. Quaternary Research 10, 310-339.

Cooke, H.B.S. 1958. Observations relating to Quaternary environments in east and southern Africa. Transactions of the Geological Society of South Africa 61, 73.

Duller, G.A.T. 1994. Luminescence dating of sediments using single aliquots - new procedures. Quaternary Geochronology 13, 149-156.

Eitel, B. and Blumel, W.D. 1998. Pans and dunes in the southwestern Kalahari (Namibia): geomorphology and evidence for Quaternary palaeoclimates. Zeitschrift für Geomorphologie NF Supplement-band 111, 73-95.

Haddon, I. 1999. Isopach map of the Kalahari Group, 1:2,500,000. Council for Geoscience, South Africa.

Kohfield, K.E., and Harrison, S.P. 2000. How well can we simulate past climates? Evaluating the models using global palaeoenvironmental datasets. Quaternary Science Reviews 19, 321-346.

Lancaster, N. 1981. Paleoenvironmental implications of fixed dune systems In southern-Africa. Palaeogeography, Palaeoclimatology, Palaeoecology 33, 327-346.

Lawson, M.P. 1998. Environmental change in South Africa: a luminescence based chronology of Late Quaternary lunette dune development. Unpublished PhD thesis, University of Sheffield. 249p.

Lawson, M.P. and Thomas, D.S.G. 2002. Late Quaternary lunette dune sedimentation in the southwestern Kalahari desert, South Africa: luminescence based chronologies of aeolian activity. Quaternary Science Reviews 21, 825-836.

Livingstone, I., Bullard, J.E., Wiggs, G.F.S. and Thomas, D.S.G. 1999. Grain size variations on dunes in the south-west Kalahari, southern Africa. Journal of Sedimentary Research 69, 546-552.

Marret, F., Scourse, J.D., Versteegh, G., Jansen, J.H.F. and Schneider, R. 2001. Integrated marine and terrestrial evidence for abrupt Congo palaeodischarge fluctuations during the last deglaciation. Journal of Quaternary Science 16, 761-766.

Murray, A.S. and Wintle, A.G. (2000). Luminescence dating of quartz using an improved single-aliquot regenerative-dose protocol. Radiation Measurements 32, 57-73.

Murray, A.S., Roberts, R.G. and Wintle, A.G. (1997). Equivalent dose measurement using a single aliquot of quartz. Radiation Measurements 27, 171-184.

Nicholson, S.E. 2000. The nature of rainfall variability over Africa on time scales of decades to millennia (sic). Global and Planetary Change 26, 137-158.

O'Connor, P.W. and Thomas, D.S.G. 1999. The timing and environmental significance of Late Quaternary linear dune development in western Zambia. Quaternary Research 52, 44-55.

Olley, J.M., Murray, A. and Roberts, R.G. (1996). The effects of disequilibria in the uranium and thorium decay chains on burial dose rates in fluvial sediments. Quaternary Science Reviews 15, 751-760.

Partridge, T.C., Demenocal, P.B., Lorentz, S.A., Paiker, M.J., Vogel, J.C. 1997. Orbital forcing of climate over South Africa: a 200,000-year rainfall record from the Pretoria salt pan. Quaternary Science Reviews 16, 1125-1133.

Partridge, T.C., Scott, L. and Hamilton, J.E. 1999. Synthetic reconstructions of southern African environments during the Last Glacial Maximum (21-8

kyr) and the Holocene Altithermal (8-6kyr). Quaternary International 57/58, 207-214.

Peyron, O., Jolly, D., Bonnefille, R., Vincens, A. and Guiot, J. 2000. Climate of East Africa 6000 B.P. as inferred from pollen data. Quaternary Research 54, 90-101.

Prescott, J.R. & Hutton, J.T. 1994: Cosmic ray contributions to dose rates for luminescence and ESR dating: large depths and long-term time variations. Radiation Measurements 23, 497-500.

Singhvi, A.K, Banerjee, D., Ramesh, R., Rajaguru, S.N. and Gogte, V. 1996. A luminescence method for dating 'dirty' pedogenic carbonates for paleoenvironmental reconstruction. Earth and Planetary Science Letters 139, 321-332.

Singhvi, A.K and Wintle A.G. 1999. Luminescence dating of aeolian and coastal sand and silt deposits: applications and implications. In Goudie, A.S., Livingstone, I. And Stokes S. (Eds): Aeolian Environments, Sediments and Landforms, John Wiley & Sons.

Stokes, S., Thomas, D.S.G and Washington, R. 1997a. Multiple episodes of aridity in southern Africa since the last interglacial period. Nature 388, 154-158.

Stokes, S., Thomas, D.S.G. and Shaw, P.A. 1997b. New Chronological evidence for the nature and timing of linear dune development in the south west Kalahari Desert. Geomorphology 20, 81-93.

Stokes, S., Colls, A.E.L., Fattahi, M. and Rich, J. (2000). Investigations of the performance of quartz single aliquot D_E determination procedures. Radiation Measurements, 32, 585-594.

Thomas, D.S.G. and Shaw, P.A. 1991. The Kalahari Environment. CUP, Cambridge, 284p.

Thomas, D.S.G. and Shaw, P.A. 2003. Late Quaternary environmental change in central southern Africa: new data, synthesis, issues and prospects. Quaternary Science Reviews, 21, 783-797.

Thomas, D.S.G., Stokes, S. and Shaw, P.A. 1997. Holocene aeolian activity in the south western Kalahari Desert, southern Africa: significance and relationships to late-Pleistocene dune-building events. The Holocene 7, 273-281.

Thomas, D.S.G., O'Connor, P.W., Bateman, M.D., Shaw, P.A., Stokes, S., Nash, D.J. 2000. Dune activity as a record of late Quaternary aridity in the Northern Kalahari: new evidence from northern Namibia interpreted in the context of regional arid and humid chronologies. Palaeogeography, Palaeoclimatology, Palaeoecology 156, 243-259.

Thomas, D.S.G., Brooks, G., Shaw, P., Bateman, M.D., Haberyan, K., Appleton, C., Nash, D. McClaren, S. and Davies, F. (2003). Late Pleistocene wetting and drying in the NW Kalahari: an integrated study from the Tsodilo Hills, Botswana. Quaternary International 104, 53-67.

Tyson, P.D. 1986. Climate Change and variability in Southern Africa. Oxford University Press, Oxford, 220p.

Williams, I.I.E. 1993. Geological summary of the Kalahari Formation in the north west boundary of Mamatwan Open Pit. Internal Memoir, Samancor, Hotazel.

Bateman *et al.* (2003) as published in Quaternary International 111 (2003) 37–49